OPTOELECTRONICS AND ADVANCED MATERIALS – RAPID COMMUNICATIONS Vol. 9, No. 9-10, September – October 2015, p. 1190 - 1193

# A comparative study of $Cu_2MnSnS_4$ thin films synthesized via different chemical methods

XU WANG*, TIANTIAN LIU, HAO GUAN, FANGLI YU, HAIJUN HOU
*School of Materials Engineering, Yancheng Institute of Technology, 9 Yinbing Street, Yancheng 224051, PR China*

Quaternary $Cu_2MnSnS_4$ (CMTS) thin films were synthesized via three different chemical methods. The as-obtained CMTS thin films were characterized by X-Ray diffraction, scanning electron microscopy and UV-vis-NIR absorbance spectroscopy measurements. The CMTS thin films exhibit the polycrystalline nature of the CMTS films with stannite structure. From the scanning electron microscopy images, CMTS thin films are found to have different morphologies. The optical band gap values are estimated to be 1.15, 1.26 and 1.17eV, respectively. All CMTS thin films show *p* type semiconductor material characteristic. The results indicate that the as-obtained CMTS thin films are a potential candidate for application as absorber layer in thin film solar cells.

(Received October 29, 2014; accepted September 9, 2015)

*Keywords*: Thin films, $Cu_2MnSnS_4$, Chemical method, Sulfurization

## 1. Introduction

In recent years, chalcopyrite semiconductors attract a great deal of interests due to their suitable band gaps and high optical absorption coefficient for potential application in thin film solar cells [1-2]. Recently, the high power conversion efficiencies of solar cells based on $Cu_2ZnSnS_4$ (CZTS) and $Cu_2ZnSn(S, Se)_4$ as high as 8.4% and 11.1% have been reported [3-4]. Because of its similar structure to CZTS, a class of quaternary chalcogenides such as $Cu_2FeSnS_4$, $Cu_2CdSnS_4$, $Cu_2MnSnS_4$ (CMTS), $Cu_2CoSnS_4$ and $Cu_2NiSnS_4$ has been receiving attention, and the structures and properties have also been studied [5-11]. Several methods based on vacuum and non-vacuum techniques have been developed for fabrication of chalcopyrite compounds. Compared to vacuum techniques, non-vacuum techniques including sol-gel, electro-deposition, chemical bath deposition(CBD), successive ionic layer absorption and reaction (SILAR) and ink printing are promising ones due to simpleness, low-price and no-need of sophisticated instrumentation. To the best of our knowledge, the fabrication of $Cu_2MnSnS_4$ thin film has rarely been reported. Here we report on three different chemical methods for preparing CMTS thin films on glass substrates. The structure, morphology, optical and electrical properties of the films were also investigated.

## 2. Experimental details

Before the deposition of the precursor film, the glass substrate was firstly ultrasonically cleaned by acetone and then ultrasonically cleaned by de-ionized water.

The CMTS thin films can be obtained by sulfurizing different precursor (Cu,Sn)S/MnS and (Cu,Sn,Mn)S films. The precursor films were deposited by three chemical methods: (a) For the deposition of (Cu,Sn)S layer, A mixed solution of $SnCl_2$ (0.03M) and $CuCl_2$ (0.06M) was used as the cationic precursor solution, and $Na_2S$ (0.12M) solutions were used as the anionic precursor solution. A glass substrate was immersed in the cationic precursor solution. After that the substrate was rinsed with de-ionized water to remove unabsorbed $Sn^{2+}$ ions and $Cu^{2+}$ ions from the substrate. Then the substrate was immersed in anionic precursor. Further, rinsing again in de-ionized water to remove loose material from the substrate was followed. For the deposition of MnS layer on the (Cu,Sn)S layer, $Mn(CH_3COO)_2$ (0.03M) solutions and $Na_2S$ (0.12M) solutions were used as the cationic precursor solution and as the anionic precursor solution, respectively. The number of immersion cycles for (Cu,Sn)S and MnS layers was 60. (b) For the deposition of (Cu,Sn)S layer, A mixed solution of $SnCl_2$ (0.03M) and $CuCl_2$ (0.06M) was used as the cationic precursor solution, and $Na_2S$ (0.12M) solutions were used as the anionic precursor solution. The number of immersion cycles for (Cu,Sn)S layer was 60. For the deposition of MnS layer on the (Cu,Sn)S layer, $Mn(CH_3COO)_2$ (0.04M), $C_6H_5Na_3O_7$ (0.06M), $NH_4Cl$ (0.06M) and thiourea (0.12M) were added in de-ionized water. Clear solution was formed after being stirred at room temperature for ten minutes, then proper ammonia were added to adjust the pH value of the deposition solution. After this, A glass substrate with the layer of (Cu, Sn)S was inserted into the solution, and the deposition takes place at 60 ℃ for 5 h. (c) For the deposition of (Cu,Sn,Mn)S layer, A mixed solution of

$SnCl_2$ (0.03M), $Mn(CH_3COO)_2$ (0.03M)and $CuCl_2$ (0.06M) was used as the cationic precursor solution, and $Na_2S$ (0.12M) solutions were used as the anionic precursor solution. The number of immersion cycles for (Cu,Sn,Mn)S layer was 60.

After the deposition, the precursor films were rinsed by de-ionized water and collected. Then they were annealed at 500 °C for 1h. During the annealing, the precursor was kept in an atmosphere of nitrogen and sulfur vapor.

The structure studies were carried out using a PANalytical X'Pert PRO diffractometer (XRD) with Cu $K_\alpha$ radiation (λ=0.15406 nm). The microstructure was recorded using LEO-1530VP scanning electron microscope (SEM). The optical characteristics were measured using Varian Cary 5000 spectrophotometer to calculate band gap energy. The electrical properties were evaluated using Hall measurements.

## 3. Result and discussion

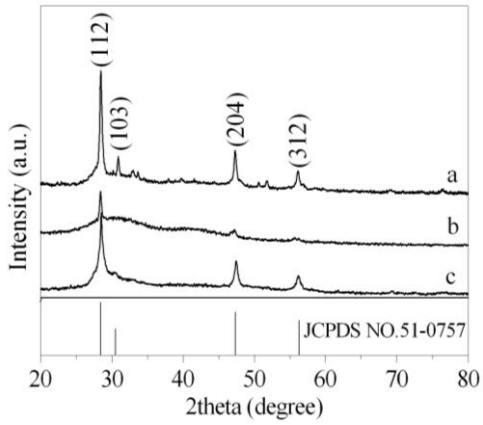


*Fig. 1. X-ray diffraction patterns of the as-synthesized CMTS films*

The XRD patterns of the as-obtained CMTS samples (a, b, c) are shown in Fig.1. Where samples (a, b, c) are the ones obtained by three chemical methods (a, b, c). We can see that the patterns of the samples match well with the stannite structure of the CMTS samples (JCPDS NO.51-0757). The main diffraction peaks appeared at $2\theta$=28.3°, 29.8°, 47.1° and 55.8° can be attributed to the (112), (103), (204) and (312) plans of CMTS, respectively. No other characteristic peaks from other crystalline forms are detected, indicating that no secondary phases were present. The average grain sizes ($D$) can be calculated from X-Ray diffractions at grazing incidence using Debye-Scherrer formula:

$$D = \frac{0.94\lambda}{\beta\cos\theta} \tag{1}$$

Where $\lambda$ is the wavelength of X-ray radiation,$\theta$ is the Bragg's angle of the 112 peak,and $\beta$ is the angular width of the peak at full width at half maximum (FWHM). The values are about 18nm, 14nm and 22nm, respectively. According to $2\theta$ and FWHM ($\beta$) of the related peak, we can calculate micro-strain ($\varepsilon$) and dislocation density ($\rho$). The corresponding formulas are given below [12-13]:

$$\varepsilon = \frac{\beta\cos\theta}{4} \tag{2}$$

$$\rho = \frac{1}{D^2} \tag{3}$$

The estimated values are shown in Table1. It can be seen that sample b has the highest micro-strain and dislocation density among three samples. It is due to the different growth processes of the grown SILAR (Cu,Sn)S layer and the grown CBD MnS layer for sample b.

*Table 1. Estimated structural parameters of the as-synthesized CMTS films*

.

| Sample | Average grain size($D$) (nm) | Micro-strain ($\varepsilon$)×$10^{-4}$ | Dislocation density ($\rho$) ×$10^{15}$ ($m^{-2}$) |
|---|---|---|---|
| a | 22 | 16 | 2.1 |
| b | 14 | 26 | 5.1 |
| c | 18 | 20 | 3.1 |

Fig.2 shows the SEM images of the as-obtained CMTS samples. It is evident that the surface morphologies of sample a and sample c exhibit flower-like structure with self-assembly flaky particles while irregular crystalline grains with a few voids are observed in sample b. It is maybe caused by the growth mechanism of MnS layer, exhibiting ion-by-ion mechanism and hydroxide cluster mechanism for sample a, c and sample b, respectively. We also noticed that sample a have larger flaky particles than sample c, in accordance with XRD analysis.

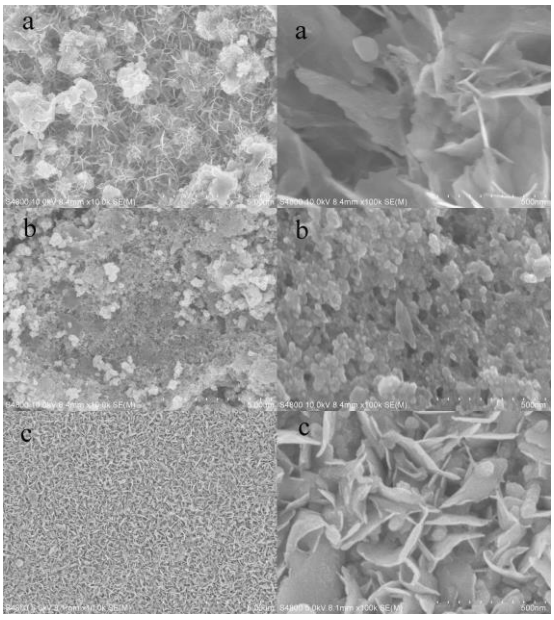


*Fig. 2. SEM images of the as-synthesized CMTS films with low and high magnifications.*

The optical band gaps can be estimated from the $(\alpha h\nu)^2$ versus $h\nu$ graph, where $\alpha$ is the absorption coefficient, $h\nu$ is the photon energy, by extrapolating the linear absorption edge part of the curve to the intersection with energy axis. Fig. 3 gives the optical band gap energies of the as-obtained CMTS samples. It can be seen that the direct optical band gap energies are estimated to be 1.15, 1.26 and 1.17eV for sample a, b and c, respectively. It can be said that the $E_g$ values are near to the optimum band gap for solar cells, indicating suitable optical properties for solar cell applications. From SEM images in Fig. 2, we can see that the direct band gap increases with the decreases in the crystallite size. It is due to quantum confinement effect [14].

Table 2 shows the electrical properties of the as-obtained CMTS samples. The variety of the carrier concentrations is not considerable, indicating the phases of the as-obtained CMTS samples are uniform. So the mobility of CMTS films was dependant on the microstructure of thin films [15]. Sample b shows low electrical mobility due to the existence of voids. The electrical mobility of sample a is larger than the one of sample c because crystalline grains are improved. In addition, all CMTS films exhibit *p* type semiconductor material characteristic.

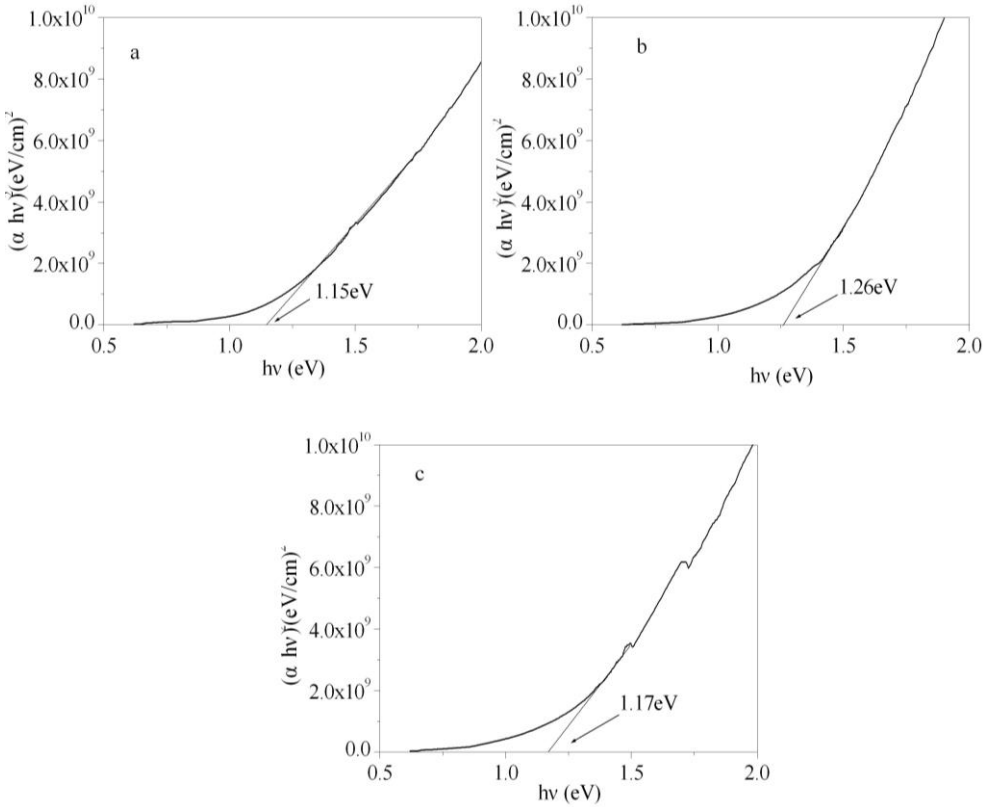


*Fig. 3. Optical band gap estimation of the as-synthesized CMTS films.*

*Table 2. Carrier concentration and mobility of the as-synthesized CMTS films.*

| Sample | Carrier concentration($cm^{-3}$) | Mobility($cm^2$/VS) |
|---|---|---|
| a | $4.98\times10^{18}$ | 46.84 |
| b | $4.71\times10^{18}$ | 5.38 |
| c | $4.82\times10^{18}$ | 32.77 |

## 4. Conclusions

In summary, CMTS thin films were synthesized via three different chemical methods. The XRD studies indicate the polycrystalline nature of the CMTS films with stannite structure. No other secondary phases are detected. The grain sizes of the films via three different chemical methods are calculated to be about 18nm, 14nm and 22nm, respectively. From the scanning electron microscopy images, the different CMTS thin films exhibit different morphologies due to different growth processes. The optical band gap values were estimated to be 1.15, 1.26 and 1.17eV, respectively. From Hall measurement, All CMTS thin films show *p* type semiconductor material characteristic. The results indicate that the as-synthesized CMTS films are suitable for solar cell applications.

**Acknowledgement**

This research is financial supported by the National Natural Science Foundation of China (No.51202211 and No. 51402251).

## References

[1] H. Katagiri. Thin Solid Films **426**, 480 (2005).
[2] J. Tang, S. Hinds, S. O. Kelley, E. H. Sargent, Chem. Mater. **20**, 6906 (2008).
[3] B. Shin, O. Gunawan, Y. Zhu, N. A. Bojarczuk, S. J. Chey, S. Guha., Prog. Photovolt. Res. Appl. **21**, 72 (2013).
[4] T. K. Todorov, J. Tang, S. Bag, O. Gunawan, T. Gokmen, Y. Zhu, D. B. Mitzi, Adv. Energy Mater. **3**, 34 (2013).
[5] X. Zhang, N. Bao, K. Ramasamy, Y. H. A. Wang, Y. Wang, B. Lin, A. Gupta, Chem. Commun. **48**, 4956 (2012).
[6] L. H. Ai, J. Jiang, J. Mater. Chem. **22**, 20586 (2012).
[7] C. Yan, C. Huang, J. Yang, F. Liu, J. Liu, Y. Lai, J. Li, Y. Liu, Chem. Commun. **48**, 2603 (2012).
[8] X. Jiang, W. Xu, R. Q. Tan, W. J. Song, J. M. Chen, Mater. Lett. **102**, 39 (2013).
[9] Y. Cui, G. Wang, D. C. Pan, J. Mater. Chem. **22**, 12471 (2012).
[10] M. Cao, L. Li, W. Z. Fan, X. Y. Liu, Y. Sun, Y. Shen, Chem. Phys. Lett. **534**, 34 (2012).
[11] Y. Cui, R. P. Deng, G. Wang, D. C. Pan, J. Mater. Chem. **43**, 23136 (2012).
[12] R. Sathyamoorthy, C. Sharmila, K. Natarajan, S. Velumani, Mater.Charact. **58**, 745 (2007).
[13] S. Kahraman, S. Çetinkaya, H. A. Çetinkara, H. S. Güder, Thin Solid Films **550**, 36 (2014).
[14] K. Moriya, J. Watabe, K. Tanaka, H. Uchiki, Phys. Status Solidi C **3**, 2848 (2006).
[15] M. Ikhlasul Amal, K. H. Kim, J. Mater. Sci: Mater. Electron. **24**, 559 (2013).

*Corresponding author: wangxuycit@sina.com